Termodynamics and kinetics for the evolution of non-metallic inclusions in pipeline steel

Y. Zhang, Y. Ren, L. Zhang

In the current study, the thermodynamics for the complex deoxidation of the pipeline steels was established and discussed, comparing to the deoxidation of pure iron. A remarkable difference in the deoxidation curve bretween real pipeline steel and pure iron was found since for real steels complex inclusions, such as calcium-aluminate, alumina and sulfide, were generated during deoxidation rather than pure alumina with the increasing of the dissolved aluminum in steel. A kinetic model was developed to predict the composition variation with time of non-metallic inclusions, steel and slag during LF refining of pipeline steels. Reactions between alloy elements and steel generating inclusions, slag and steel, between slag and lining refractory, between steel and lining refractory were considered in this kinetic model, considering air absorption and the removal of inclusions. The effects of inclusion size and gas flow rate during LF refining on the composition variation with time of inclusions, steel and slag were investigated. The kinetic model showed a good agreement with industrial measurement of the composition of inclusions, steel and slag.

KEYWORDS: THERMODYNAMICS – KINETICS – EVOLUTION – NON-METALLIC INCLUSIONS – PIPELINE STEELS

INTRODUCTION

The composition, size, number, and distribution of inclusions in linepipe steels have a huge influence on the performance the linepipe steels. [1, 2] The solid inclusions may cause the clogging of the submerged entry nozzle.[3-5] The indeformable inclusions in linepipe steels can lead to the hydrogen induced cracking.[6-8] The control of inclusions is the key task of the steelmakers. There have been a large number of studies on the control of inclusions by lab experiments and plante trials.[9] Traditionally, it is suggested that inclusions in linepipe steels should be modified to liquind calcium aluminates at steelmaking temperature.[10, 11] Meanwhile, the modification machnism of the Al_2O_3 inclusions in Al-killed steel was widely investigated. It is found that the Al_2O_3 inclusions were directly reduced by dissolved calcium or indirectly reduced via CaO formed from [Ca] and [O]. Inversely, it is also reported that CaS phase in inclusions are transiently formed immediately after the calcium addition, then decreases and disappears. [12-16] However, it is found that the fully liquid CaO-Al_2O_3 are in large size and easier to be rolled to stringer shaped inclusions.[17] Thus, to avoid the formation of the liquid CaO-Al_2O_3 inclusions, it is proposed that adding the insufficient or superfluous calcium can modify inclusions to partially liquid CaO-Al_2O_3 inclusions, which can hardly lead to the nozzle clogging and the formation of the hydrogen induced cracking. To achieve the better controlling of inclusion composition after the reaction equilibium, many efforts has been carried out to predict the deoxidation and inclusion formation in liquid pure iron by thermodynamic calculation.The deoxidation equilibrium relationship by single deoxidizer could be maturely predicted by thermodynamic calculation, such as Al-O[18, 19], Mg-O[20], Ca-O[21, 22], etc. The thermodynamic data of alloy elements in the molten steel were summarized and suggested by JSPS.[23] To predict the formation of complex inclusions such as Mg-Al-O, Al-Ti-O, Al-Ca-O, Al-Si-O, Mg-Al-Ca-O, etc., the experimets and thermodynamic calculation for the pure iron with the addition of multi-deoxidizers have been conducted.[24-29] Especially, the application of thermodynamic databases was introduced to steelmaking process[30, 31],

Ying Zhang, Ying Ren, Lifeng Zhang
School of Metallurgical and Ecological Engineering,
University of Science and Technology Beijing
Beijing 100083, China
email: zhanglifeng@ustb.edu.cn

which significantly improve the accuracy of the thermodynamic prediction. However, most of the previous studies focus on the inclusion formation in the liquid iron, insteady of the real steel. Thus, the thermodynamics for the complex deoxidation of the pipeline steels was established and discussed in the current study.

To precisely predict composition variation with time of non-metallic inclusions, steel, and slag, some kinetic model has been developed. Harada et al[32-34] developed a kinetic model to calculate composition changes in the molten steel, the slag, and the inclusion in ladle refining. The coupled reaction model was applied to the reaction between the molten steel/slag phase and the molten steel/inclusion originating from the slag. Empirical equations were used to calculate the rate of MgO dissolution in the slag from the refractory. Peter et al developed a model to model and simulate the ladle refining at two different LMF's, refining Al-killed and Si-deoxidized steels using the process simulation program Metsim and the thermodynamical program FactSage.[35] A comprehensive model for inclusion development in gas stirred ladles developed by the Shu and Scheller, which is a useful tool for simulation and optimization of ladle metallurgical treatments in industry.[36] Jung et al applied a the effective equilibrium reaction zone model using the FactSage macro processing code to develop a kinetic LF process model.[37] Shin et al developed a refractory–slag–metal–inclusion multiphase reaction model by integrating the refractory–slag, slag–metal, and metal–inclusion elementary reactions in order to predict the evolution of inclusions during the secondary refining processes.[38] Piva et al simulated steel-slag and steel-inclusion reaction kinetics in silicon-manganese killed steels using FactSage macros.[39] Ying et al developed kinetic models using FactSage Macro Processing to simulate the composition evolutions of slag, steel, and inclusions during the calcium treatment, slag refining, and reoxidation processes.[40-43]

In the current study, a kinetic model was developed to predict the composition variation with time of non-metallic inclusions, steel and slag during LF refining of pipeline steels with the consideration of reactions between alloy elements and steel generating inclusions, slag and steel, between slag and lining refractory, between steel and lining refractory

THERMODYNAMICS FOR INCLUSIONS IN PIPELINE STEELS

The formed typical inclusions in linepipe steels are shown in Fig.1. During the production prcess of linepipe steels, the Al_2O_3 inclusions formed after the Al deoxidation. As the reduction of MgO in slag and refractory, the Mg transfers to the moten steel and react with the inclusions. The formed typical $MgO{\cdot}Al_2O_3$ inclusion is shown in Fig.1(a). After the modification of the slag refining and the calcium treatment, the inclusions are modified to liquid calcium aluminate at steelmaking temperature, as shown in Fig.1(b). Fig.2 shows the equilibrium relation of oxygen and aluminum contents in steel at 1873 K. In Fig.2(a) shows the Al-O curve in pure iron at 1873 K. With an increase of Al in the liquid iron, the Al content decreases first and then goes up. The minimum concentration of O in the liquid iron can be lowered to 3 ppm. Fig.2(b) shows the Al-O curve in the linepipe steel at 1873 K. The oxygen content can be decreased to several ppm with the addition of Al. The formed inclusions are solid $2CaO{\cdot}SiO_2$ with less than 0.01% Al, while the inclusions are liquid at steelmakine temperature with more than 0.01% Al. There is an obvious difference in liquind iron and the linepipe steels, as shown in Figs.2(a) and (b).

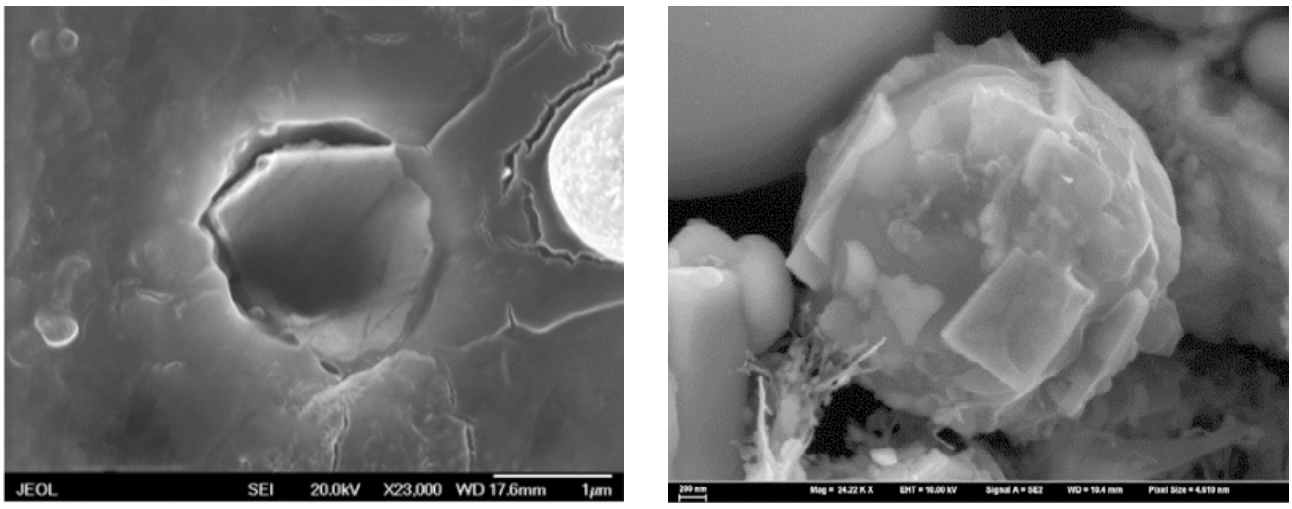

(a) $MgO{\cdot}Al_2O_3$ (b) $CaO{\cdot}Al_2O_3$

Fig. 1 – The formed $MgO{\cdot}Al_2O_3$ and $CaO{\cdot}Al_2O_3$ inclusions in linepipe steels.

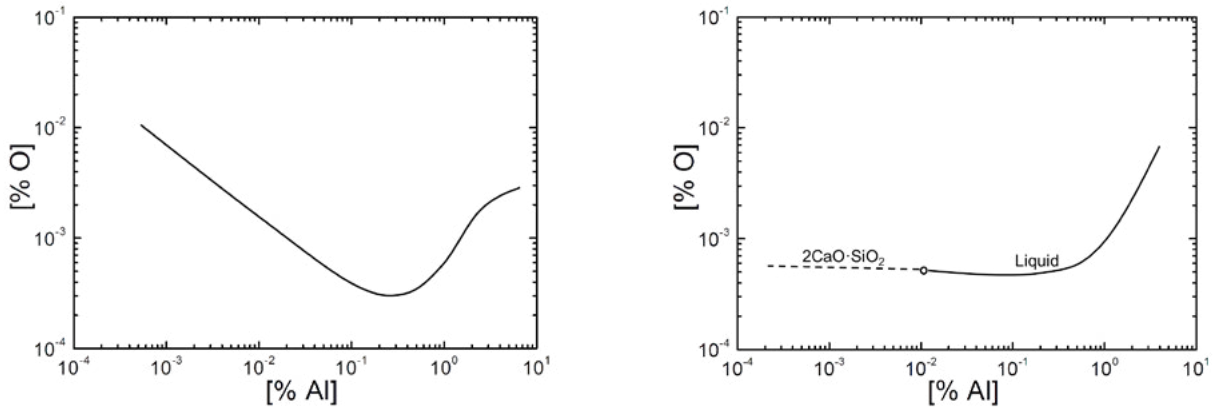

(a) Al-O curve in pure iron. [9]

(b) Al-O curve in linepipe steels. [15]

Fig. 2 – The equilibrium relation of oxygen and aluminum contents in pure iron and linepipe steels at 1873 K.

Fig.3 (a) shows the equilibrium relation of oxygen and calcium contents in pure iron under various S concentrations at 1873 K. With the increase of Ca in liquid iron, the oxygen content decrease first, then goes up. The oxygen content can be lowered to 2 ppm. The addition of S lowers the deoxidation ability of the Ca in liquid iron. Fig.3 (b) is the equilibrium of Ca-O curve in linepipe steels at 1873 K using Factsage with the FactPS and FToxid and FTmisc databases. The evolution route of oxide phase is $CaO{\cdot}6Al_2O_3 \rightarrow CaO{\cdot}2Al_2O_3 \rightarrow$ liquid inclusion $\rightarrow$ CaO. The oxygen can be decreased to roughly 5 ppm. With S increasing from 0 ppm to 200 ppm, there is a slight decrease of the oxygen content due to the transformation of the formed oxides. Since the interaction between O and S is much smaller than that between Ca and O , the relationship of the equilibrated oxygen content and the calcium content could hardly be influenced by S content.[44]

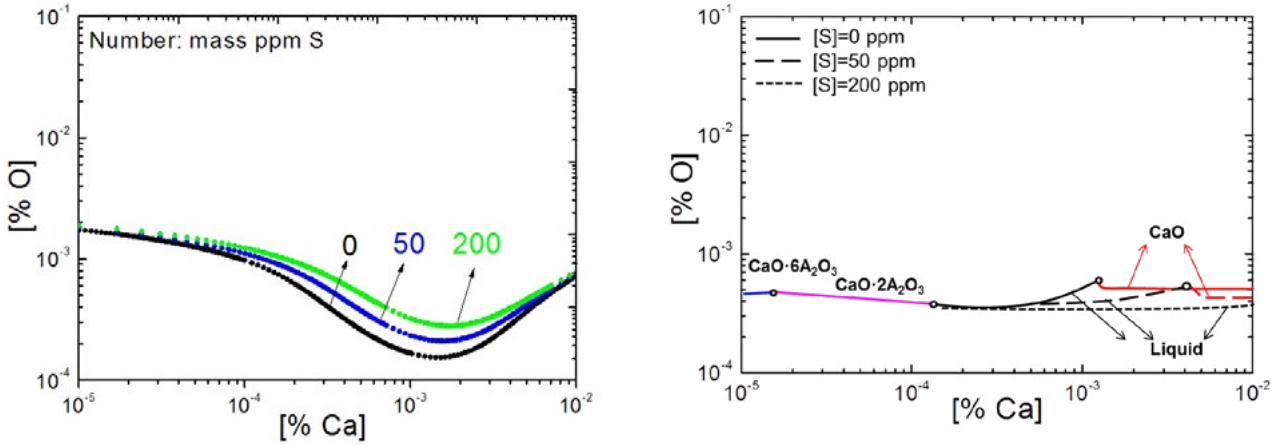

(a) Ca-O curve in pure iron. [9]

(b) Ca-O curve in linepipe steels. [15]

Fig. 3 – The equilibrium relation of oxygen and calcium contents in pure iron and linepipe steels at 1873 K.

The effect of oxygen content on the equilibrium of sulphur and calcium contents in steel at 1873 K is shown in Fig.4. Fig.4 (a) shows the Ca-S curve in pure iron with various O. It can be seen that the S content decreases with the increasing Ca in liquind iron. Meanwhile, the S content obviously increases with the increasing O content in the liquid iron. Meanwhile, the Ca-S curve in pure iron is shown in Fig.4 (a). In linepipe steels, the addition of Ca can significantly decrease the S content. As the dissolved oxygen increases, the desulphurization ability of calcium is weakened obviously. The inflection points mainly caused by the oxide phase transformation. It can be inferred that the O content has a huge influence on the equilibrium relationship between sulphur and calcium contents in the molten steel.

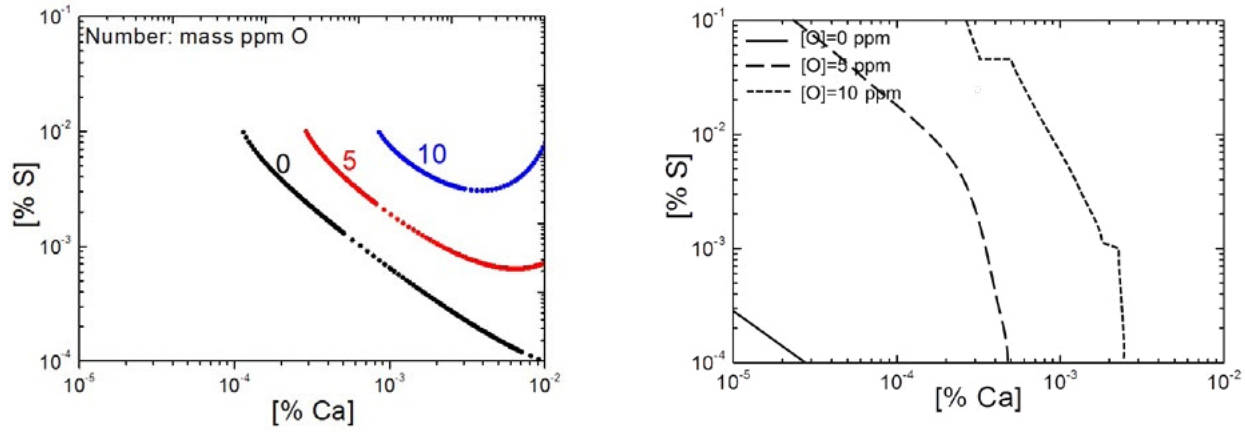

(a) Ca-S curve in pure iron. [9]

(b) Ca-S curve in linepipe steels. [15]

Fig. 4 – The equilibrium relation of oxygen and calcium contents in pure iron and linepipe steels at 1873 K.

The calculated stability diagram of Al-Ca-O system in the pure iron at 1873K is shown in Fig.5(a).[28] The formation of Al_2O_3, $CaO{\cdot}6Al_2O_3$, $CaO{\cdot}2Al_2O3$, $CaO{\cdot}Al_2O_3$, liquid calcium aluminates, and CaO nclusion phases are considered in the current calculation. The Al_2O_3 and CaO are severally formed in the pure iron with additions of superfluous O and Ca. The calcium aluminates are formed between Al_2O_3 and CaO inclusions region. Fig.4 (b) shows the calculated Al-Ca-O inclusion diagram in linepipe steels at 1873K.[15] With the addition of Ca in linepipe steels, the inclusions evolve from Al_2O_3 to $CaO{\cdot}6Al_2O_3$ to $CaO{\cdot}2Al_2O_3$, liquid calcium aluminates. The CaS and $2CaO{\cdot}SiO_2$ are formed with the superfluous Ca. A remarkable difference in the deoxidation curve bretween real pipeline steel and pure iron was found since for real steels complex inclusions, such as calcium-aluminate, alumina and sulfide, were generated during the deoxidation rather than pure alumina with the increasing of the dissolved aluminum in steel.

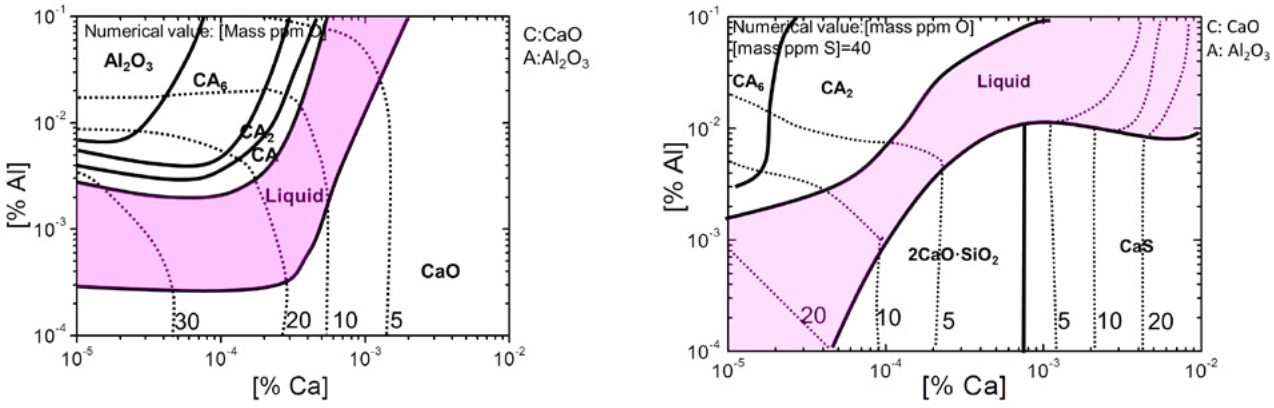

(a) Pure iron[28]

(b) Linepipe steels[15]

Fig. 5 – Stability diagram of inclusions in Al-Ca-killed steel.

KINETICS FOR EVOLUTION OF INCLUSIONS IN PIPELINE STEELS

The basic reactions between steel-slag-refractory-alloy-inclusion-air during refining process was decribed in the previous study, as the schematic diagram shown in Fig. 6.[45] The reactions of stee-slag, slag inclusions, alloy-steel, air-steel, refractory-steel, refractory-slag are considered in the current model. The reactions and the thermodynamic data can be found in our previous work. The reactions at interface were assumed to be equilibrated at any time. Then, the mass transfer is the rate-controlling step. Therefore, the reaction rate is mainly determined by the mass transfer coefficients.

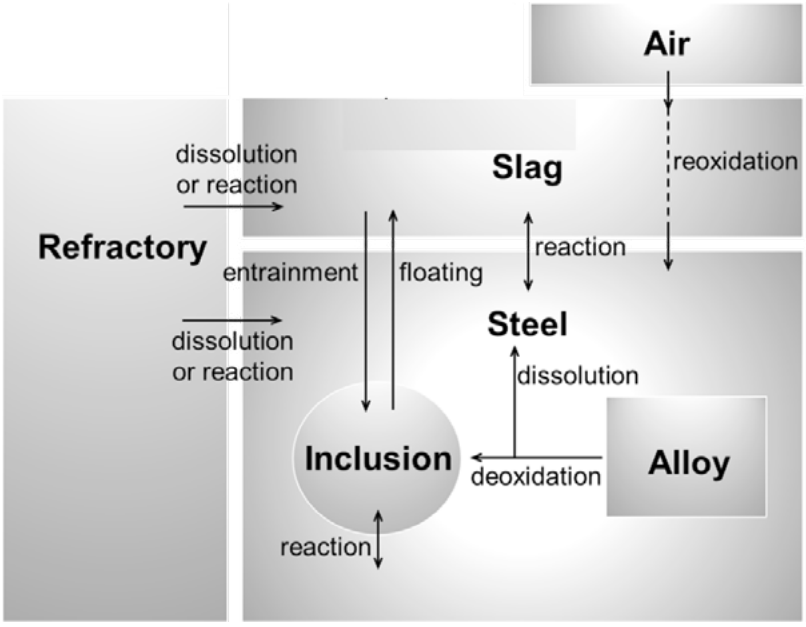

Fig. 6 – Schematic diagram of multiphase reactions during refining process[45]

In the current kinetic model, the empirical equations of the mass transfer coefficient calculation were corrected as following Eqs. [1]-[4].

$$k_m = 0.0194 \times \varepsilon^{0.688} \quad [1]$$

$$k_s = k_m / 10 \quad [2]$$

$$k_{m\_inc} = 2\left(\frac{D \cdot u_{slip}}{\pi \cdot d_p}\right)^{1/2} \quad [3]$$

$$\left.\begin{array}{ll} T > T_L, & k_{inc} = k_{m\_inc} / 10 \\ T_S < T < T_L, & k_{inc} = k_{m\_inc} / 20 \\ T < T_S, & k_{inc} = k_{m\_inc} / 100 \end{array}\right\} \quad [4]$$

where km and ks are the mass transfer coefficients of molten steel and slag, respectively, m/s; km_inc and kinc are the mass transfer coefficients of steel and inclusion during steel-inclusion reaction, m/s; ε is the effective stirring power, (W/t); T is the temperature of molten steel and inclusions, (K); D is the diffusion coefficient of elements in the molten steel, m2/s; uslip respects the relative velocity of steel and inclusion, m/s; dp is the inclusion diameter, μm; TS and TL are severally the solidus and liquidus of the inclusion, K.

A plant trial of ladle refining process of linepipe steels was simulated using the current developed model. The initial slag and steel are mainly CaO-Al_2O_3-SiO2-MgO and Al-killed linepipe steels. The initial inclusions in the molten steel are 2μm solid Al_2O_3-rich inclusions. During the refining process, the lime was added to increase the CaO in the refining slag. To validate the accuracy of the current model, the calculated and the measured T.S evolutions were compared in Fig.7. The predicted results shows a good agreement with the experimental ones, indicating that the current model can be used to predict the reactions during the ladle refining process.

Fig.8 shows the predicted evolution of slag compositions during the ladle refining process. It can be seen that there is an obvious increase in CaO content with the addition of lime. Fig.9 shows the volution of T.Ca and T.Mg during the ladle re-

fining process. It can be seen that the addtion of CaO leads to the increase of T.Ca.
Then, the T.Ca and T.Mg slowly goes down during the refining process, which may be caused by the floatation of Mg-containing inclusions. Fig.10 shows the evoltion of the CaO and Al2O3 in inclusions in the molten steel.
The initial inclusions are mainly Al_2O_3. With the slag refining process, the Al_2O_3 inclusions are modified to liquid calcium aluminate. It can be inferred that the slag refining has an obvious influence on the inclusions composition.

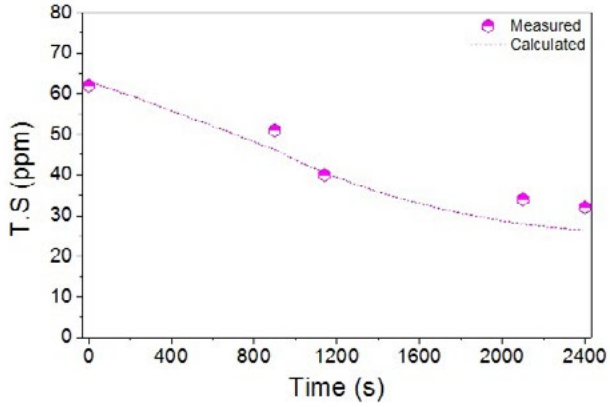

Fig. 7 – Schematic diagram of multiphase reactions during refining process

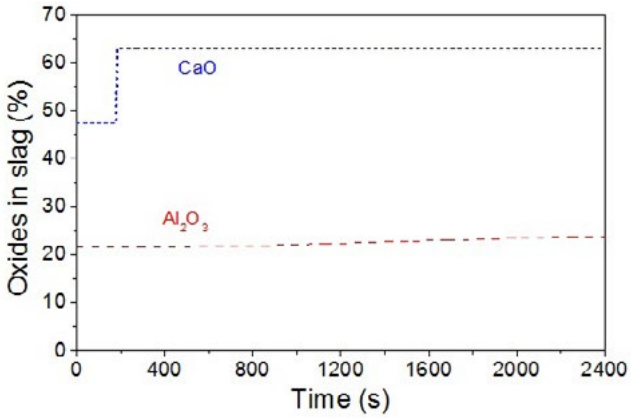

Fig. 8 – Predicted evolution of slag composition during the ladle refining process

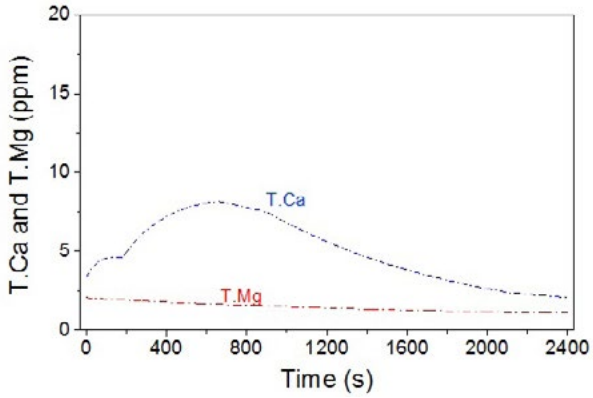

Fig. 9 – Predicted evolution of steel composition during the ladle refining process

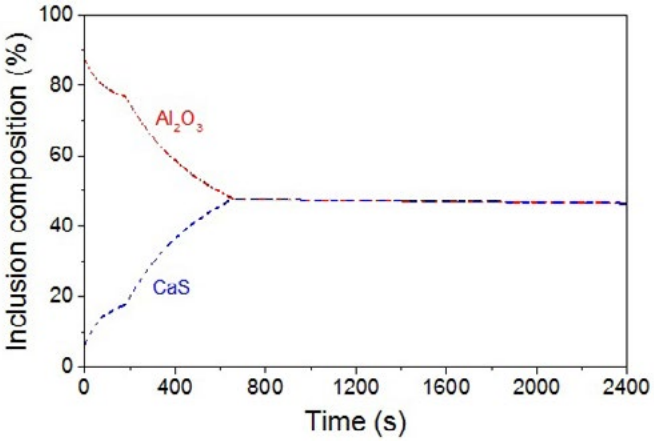

Fig. 10 – Predicted evolution of inclusion composition during the ladle refining process

To investigate the effect of inclusion size on inclusion composition evolution during the ladle refining process, the evolutions of 4.5μm, 15.5μm, and 95.5μm inclusions are compared in Fig.11. From the evolusions of Al_2O_3, CaO, and CaS in inclusions. It can bee seen that the small inclusions are modified and almost unchanged after roughly 900 seconds. However, the 95.5μm inclusions can hardly reach the equilibrium after 2400 seconds.

Meanwhile, the CaS can form by the slag refining without the calcium treatment. The MgO in inclusions slightly increases with the dissolution of MgO refractory. It is indicated that the small inclusions can be easily infuenced by the slag-steel-inclusion reactions, while the large size inclusions would keep their main composition during the refining process.

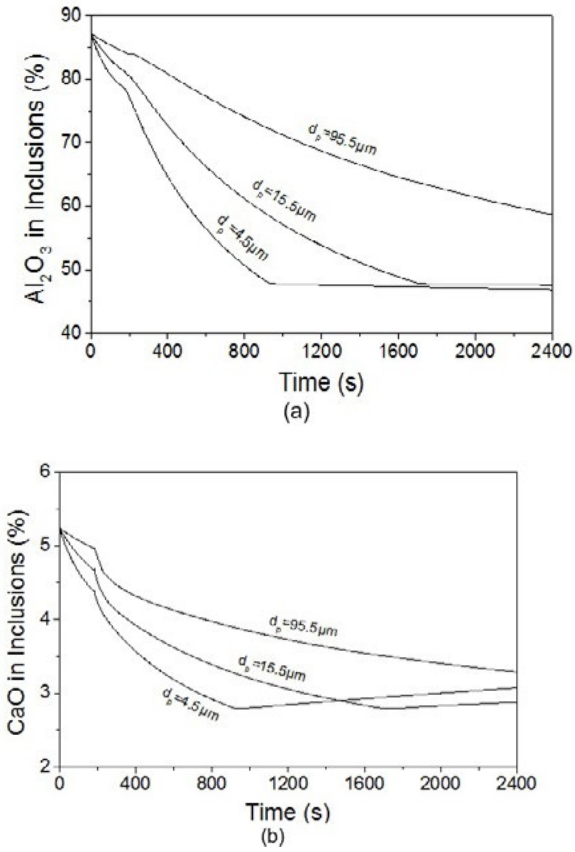

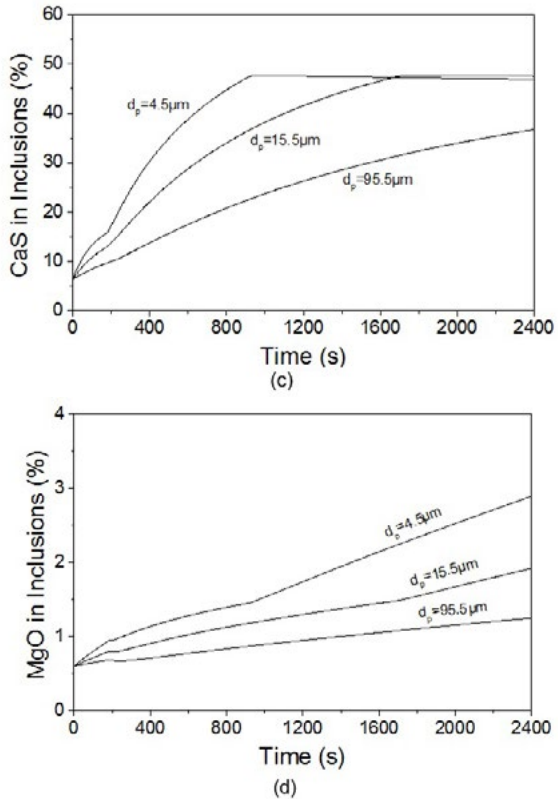

Fig. 11 – Predicted effect of inclusion size on inclusion composition evolution during the ladle refining process

CONCLUSIONS

(1) A remarkable difference in the deoxidation curve bretween real pipeline steel and pure iron was found since for real steels complex inclusions were generated during deoxidation rather than pure alumina with the increasing of the dissolved aluminum in steel.

(2) A kinetic model was developed to predict the composition variation with time of non -metallic inclusions, steel and slag during LF refining of pipeline steels. The reactions between alloy elements and steel generating inclusions, slag and steel, between slag and lining refractory, between steel and lining refractory were considered.

(3) The small inclusions can be easily infuenced by the slag-steel-inclusion reactions, while the large size inclusions would keep their main composition during the refining process.
while the large size inclusions would keep their main composition during the refining process.

ACKNOWLEDGEMENTS

The authors are grateful for support from the National Natural Science Foundation of China (Grant No. 51725402 and No. 51704018), National Postdoctoral Program for Innovative Talents (Grant No. BX201700028), Young Elite Scientists Sponsorship Program By CAST (No. 2017QNRC001), China Postdoctoral Science Foundation (No.2017M620016) and the High Quality steel Consortium (HQSC) at University of Science and Technology Beijing (USTB), China.

REFERENCES

[1] Zhang, L., State of the Art in the Control of Inclusions in Tire Cord Steels - A Review. Steel Research International, 2006. 77(3): p. 158-169.

[2] Zhang, L. and B.G. Thomas, State of the Art in Evaluation and Control of Steel Cleanliness. ISIJ International, 2003. 43(3): p. 271-291.

[3] Long, M., et al., Kinetic Modeling on Nozzle Clogging During Steel Billet Continuous Casting. ISIJ International, 2010. 50(5): p. 712-720.

[4] Vermeulen, Y., et al., Material Evaluation to Prevent Nozzle Clogging during Continuous Casting of Al Killed Steels. ISIJ International, 2002. 42(11): p. 1234-1240.

[5] Sasai, K. and Y. Mizukami, Mechanism of Alumina Adhesion to Continuous Caster Nozzle with Reoxidation of Molten Steel. ISIJ International, 2001. 41(11): p. 1331-1339.

[6] Ito, Y.-i., et al., Shape Control of Alumina Inclusions by Double Calcium Addition Treatment(Steelmaking). Tetsu-to-Hagane, 2007. 93(5): p. 355-361.

[7] Choudhary, S.K. and A. Ghosh, Thermodynamic Evaluation of Formation of Oxide-Sulfide Duplex Inclusions in Steel. ISIJ International, 2008. 48(11): p. 1552-1559.

[8] Takahashi, A. and H. Ogawa, Influence of Microhardness and Inclusion on Stress Oriented Hydrogen Induced Cracking of Line Pipe Steels. ISIJ International, 1996. 36(3): p. 334-340.

[9] Li, S., et al., Study on CaO and CaS inclusions in pipeline steel during refining process. Journal of University of Science and Technology Beijing, 2014. 36(S1): p. 168-172.

[10] Verma, N., et al., Calcium Modification of Spinel Inclusions in Aluminum-killed Steel: Reaction Steps. 2012. 43(4): p. 830-840.

[11] Yang, S., et al., Formation and Modification of MgO·Al2O3 -Based Inclusions in Alloy Steels. Metallurgical and Materials Transactions B, 2012. 43(4): p. 731-750.

[12] Verma, N., et al., Transient Inclusion Evolution During Modification of Alumina Inclusions by Calcium in Liquid Steel: Part I. Background, Experimental Techniques and Analysis Methods. Metallurgical and Materials Transactions B, 2011. 42(4): p. 711-719.

[13] Verma, N., et al., Transient Inclusion Evolution During Modification of Alumina Inclusions by Calcium in Liquid Steel: Part II. Results and Discussion. Metallurgical and Materials Transactions B, 2011. 42(4): p. 720-729.

[14] Higuchi, Y., M. Mitsuhiro, and S. Fukagawa, Inclusion Modification by Calcium Treatment. ISIJ International, 1996. 36: p. S151-S154.

[15] Ren, Y., L. Zhang, and S. Li, Transient Evolution of Inclusions during Calcium Modification in Linepipe Steels. ISIJ International, 2014. 54(12): p. 2772-2779.

[16] Yang, G. and X. Wang, Inclusion Evolution after Calcium Addition in Low Carbon Al-Killed Steel with Ultra Low Sulfur Content. ISIJ International, 2015. 55(1): p. 126-133.

[17] Yang, W., et al., Characteristics of Inclusions in Low Carbon Al-Killed Steel during Ladle Furnace Refining and Calcium Treatment. ISIJ International, 2013. 53(8): p. 1401–1410.

[18] Hayashi, A., et al., Aluminum Deoxidation Equilibrium of Molten Fe-Ni Alloy Coexisting with Alumina or Hercynite. ISIJ International, 2008. 48(11): p. 1533-1541.

[19] Kang, Y., et al., Aluminum Deoxidation Equilibrium of Molten Iron–Aluminum Alloy with Wide Aluminum Composition Range at 1873 K. ISIJ International, 2009. 49(10): p. 1483-1489.

[20] Itoh, H., M. Hino, and S. Banya, Deoxidation Equilibrium of Magnesium in Liquid Iron. Tetsu-to-Hagane, 1997. 83(10): p. 623-628.

[21] Ohta, H. and H. Suito, Deoxidation Equilibria of Calcium and Magnesium in Liquid Iron. Metallurgical and Materials Transactions B, 1997. 28(6): p. 1131-1139.

[22] Han, Q., et al., The Calcium-Phosphorus and the Simultaneous Calcium-Oxygen and Calcium-Sulfur Equilibria in Liquid Iron. Metallurgical and Materials Transactions B, 1988. 19(4): p. 617-622.

[23] Science, T.J.S.f.t.P.o., Steelmaking Data Sourcebook. Gordon and Breach Science (New York), 1988.

[24] Itoh, H., M. Hino, and S. Ban-Ya, Thermodynamics on the Formation of Spinel Nonmetallic Inclusion in Liquid Steel. Metallurgical and Materials Transactions B, 1997. 28(5): p. 953-956.
[25] Jung, I.-H., et al., Thermodynamic Modeling of the Al2O3–Ti2O3–TiO2 System and Its Applications to the Fe–Al–Ti–O Inclusion Diagram. ISIJ International, 2009. 49(9): p. 1290-1297.
[26] Itoh, H., M. Hino, and S. Banya, Thermodynamics on the Formation of Non-metallic Inclusion of Spinel (MgO·Al2O3) in Liquid Steel. Tetsu-to-Hagane, 1998. 84(2): p. 85-90.
[27] Taguchi, K., et al., Complex Deoxidation Equilibria of Molten Iron by Aluminum and Calcium. ISIJ International, 2005. 45(11): p. 1572-1576.
[28] Ren, Y., et al., Detection of Non-metallic Inclusions in Steel Continuous Casting Billets. Metallurgical and Materials Transactions B, 2014. 45(4): p. 1291-1303.
[29] Kang, Y.-B. and H.-G. Lee, Inclusions Chemistry for Mn/Si Deoxidized Steels: Thermodynamic Predictions and Experimental Confirmations. ISIJ International, 2004. 44(6): p. 1006-1015.
[30] Jung, I.-H., S. Decterov, and A. Pelton, A thermodynamic model for deoxidation equilibria in steel. Metallurgical and Materials Transactions B, 2004. 35(3): p. 493-507.
[31] Jung, I.-H., Overview of the applications of thermodynamic databases to steelmaking processes. CALPHAD: Computer Coupling of Phase Diagrams and Thermochemistry, 2010. 34(3): p. 332-362.
[32] Harada, A., et al., Kinetic Analysis of Compositional Changes in Inclusions during Ladle Refining. ISIJ International, 2014. 54(11): p. 2569-2577.
[33] Harada, A., et al., A Kinetic Model to Predict the Compositions of Metal, Slag and Inclusions during Ladle Refining: Part 2. Condition to Control the Inclusion Composition. ISIJ International, 2013. 53(12): p. 2118-2125.
[34] Harada, A., et al., A Kinetic Model to Predict the Compositions of Metal, Slag and Inclusions during Ladle Refining: Part 1. Basic Concept and Application. ISIJ International, 2013. 53(12): p. 2110-2117.
[35] Peter, J., et al. Experimental Study of Kinetic Processes During the Steel Treatment at two LMF's. in AISTech 2005 Proceeding. 2005. Charlotte, NC.
[36] Scheller, P.R. and Q. Shu, Inclusion Development in Steel During Ladle Metallurgical Treatment- A Process Simulation Model-Part: Industrial Validation. Steel Research International, 2014. 85(8): p. 1310-1316.
[37] Van Ende, M.-A. and I.-H. Jung, A Kinetic Ladle Furnace Process Simulation Model: Effective Equilibrium Reaction Zone Model Using FactSage Macro Processing. Metallurgical and Materials Transactions B, 2017. 48(1): p. 28-36.
[38] Shin, J.H., Y. Chung, and J.H. Park, Refractory–Slag–Metal–Inclusion Multiphase Reactions Modeling Using Computational Thermodynamics: Kinetic Model for Prediction of Inclusion Evolution in Molten Steel. Metallurgical and Materials Transactions B, 2017. 48(1): p. 46-59.
[39] Piva, S.P.T., D. Kumar, and P.C. Pistorius, Modeling Manganese Silicate Inclusion Composition Changes during Ladle Treatment Using FactSage Macros. Metallurgical and Materials Transactions B, 2017. 48(1): p. 37-45.
[40] Ren, Y., L.-f. Zhang, and Y. Zhang, Modeling reoxidation behavior of Al–Ti-containing steels by CaO–Al2O3–MgO–SiO2 slag. Journal of Iron and Steel Research International, 2018: p. 1-11(Published online).
[41] Ren, Y. and L. Zhang, Modeling Inclusion Evolution in Al-Ti-killed Steels during Ladle Mixing Process. Ironmaking & Steelmaking, 2017: p. Accepted.
[42] Huang, F., et al., Kinetic Modeling for the Dissolution of MgO Lining Refractory in Al-Killed Steels. Metallurgical and Materials Transactions B, 2017. 48(4): p. 1-12.
[43] Ren, Y., Y. Zhang, and L. Zhang, A kinetic model for Ca treatment of Al-killed steels using FactSage macro processing. Ironmaking & Steelmaking, 2017. 44(7): p. 497-504.
[44] Taguchi, K., et al., Deoxidation and Desulfurization Equilibria of Liquid Iron by Calcium. ISIJ Iniemational, 2003. 43(11): p. 1705–1709.
[45] Zhang, Y., Y. Ren, and L. Zhang. Kinetic variation of the composition of inclusions, steel and slag during refining of pipeline steel. in AISTech 2017 Iron and Steel Technology Conference, May 8, 2017 - May 11, 2017. 2607-2613.